The Journal of Immunology

Human Lymph Nodes Maintain TCF-1^{hi} Memory T Cells with High Functional Potential and Clonal Diversity throughout Life

Michelle Miron, Brahma V. Kumar, Wenzhao Meng, Tomer Granot, Dustin J. Carpenter, Takashi Senda, Dora Chen, Aaron M. Rosenfeld, Bochao Zhang, Harvey Lerner, Amy L. Friedman, Uri Hershberg, Yufeng Shen, Adeeb Rahman, Eline T. Luning Prak and Donna L. Farber

J Immunol published online 15 August 2018
http://www.jimmunol.org/content/early/2018/08/15/jimmunol.1800716

The Journal of Immunology is published twice each month by The American Association of Immunologists, Inc., 1451 Rockville Pike, Suite 650, Rockville, MD 20852

Print ISSN: 0022-1767 Online ISSN: 1550-6606.

Published August 15, 2018, doi:10.4049/jimmunol.1800716

Human Lymph Nodes Maintain TCF-1^{hi} Memory T Cells with High Functional Potential and Clonal Diversity throughout Life

Michelle Miron,*,† Brahma V. Kumar,* Wenzhao Meng,‡ Tomer Granot,* Dustin J. Carpenter,* Takashi Senda,* Dora Chen,‡ Aaron M. Rosenfeld,§ Bochao Zhang,§ Harvey Lerner,¶ Amy L. Friedman,¶ Uri Hershberg,§ Yufeng Shen,‖,# Adeeb Rahman,** Eline T. Luning Prak,‡ and Donna L. Farber*,†,††

Translating studies on T cell function and modulation from mouse models to humans requires extrapolating in vivo results on mouse T cell responses in lymphoid organs (spleen and lymph nodes [LN]) to human peripheral blood T cells. However, our understanding of T cell responses in human lymphoid sites and their relation to peripheral blood remains sparse. In this study, we used a unique human tissue resource to study human T cells in different anatomical compartments within individual donors and identify a subset of memory CD8$^+$ T cells in LN, which maintain a distinct differentiation and functional profile compared with memory CD8$^+$ T cells in blood, spleen, bone marrow, and lungs. Whole-transcriptome and high-dimensional cytometry by time-of-flight profiling reveals that LN memory CD8$^+$ T cells express signatures of quiescence and self-renewal compared with corresponding populations in blood, spleen, bone marrow, and lung. LN memory T cells exhibit a distinct transcriptional signature, including expression of stem cell–associated transcription factors TCF-1 and LEF-1, T follicular helper cell markers CXCR5 and CXCR4, and reduced expression of effector molecules. LN memory T cells display high homology to a subset of mouse CD8$^+$ T cells identified in chronic infection models that respond to checkpoint blockade immunotherapy. Functionally, human LN memory T cells exhibit increased proliferation to TCR-mediated stimulation and maintain higher TCR clonal diversity compared with memory T cells from blood and other sites. These findings establish human LN as reservoirs for memory T cells with high capacities for expansion and diverse recognition and important targets for immunotherapies. ***The Journal of Immunology*****, 2018, 201: 000–000.**

T cells mediate adaptive immune responses and long-lived protective immunity through their differentiation to effector and memory T cell populations, respectively. Although the majority of effector T cells are short-lived in vivo, a subset of primed effector cells differentiate and persist as populations of long-lived memory T cells. In humans, T cell subset differentiation and memory maintenance have been extensively characterized from peripheral blood, revealing subsets of memory T cells that differ in phenotype and proliferative potential (1, 2). However, the majority of T cells in the body are localized in tissue sites, particularly in lymphoid tissues, including bone marrow (BM), spleen, and an estimated 700 lymph nodes (LN) (3), where T cell responses are initiated, regulated, and maintained. How human T cells in lymphoid sites function and persist relative to subsets in blood is not well understood; defining their nature is important for monitoring and modulating immune responses and translating findings from mouse models in which T cells from spleen and LN are the predominant sites of investigation.

In human tissues, a significant fraction of memory T cells express markers, including CD69 and CD103, which denote tissue-resident memory T (TRM) (4–6). In human lymphoid tissue, a lower proportion of memory T cells express CD69 and CD103 compared with mucosal sites (4). It is not known whether lymphoid memory T cells persist with similar functional properties across tissues or adopt compartment-specific attributes. Moreover, memory T cells in secondary lymphoid organs of laboratory mice generally do not exhibit TRM phenotypes (7), suggesting that lymphoid memory T cells in humans may exhibit features distinct

*Columbia Center for Translational Immunology, Columbia University Medical Center, New York, NY 10032; †Department of Microbiology and Immunology, Columbia University, New York, NY 10032; ‡Department of Pathology and Laboratory Medicine, Perelman School of Medicine, University of Pennsylvania, Philadelphia, PA 19102; §School of Biomedical Engineering, Drexel University, Philadelphia, PA 19104; ¶LiveOnNY, New York, NY 10001; ‖Department of Systems Biology, Columbia University, New York, NY 10032; #Department of Biomedical Informatics, Columbia University, New York, NY 10032; **Icahn School of Medicine at Mount Sinai, New York, NY 10029; and ††Department of Surgery, Columbia University, New York, NY 10032

ORCIDs: 0000-0001-8991-0673 (D.C.); 0000-0002-2266-0355 (A.M.R.); 0000-0001-8968-096X (B.Z.); 0000-0002-1857-5190 (H.L.); 0000-0002-4706-8884 (A.L.F.); 0000-0002-6425-5980 (U.H.); 0000-0001-8236-9183 (D.L.F.).

Received for publication May 30, 2018. Accepted for publication July 23, 2018.

This work was supported by National Institutes of Health (NIH) Grants P01AI106697 and U19AI128949 (to D.L.F.) and NIH T32AI06711 (to M.M.). Research reported in this article was performed in the Columbia Center for Translational Immunology Flow Cytometry Core, supported by NIH Awards S10RR027050 and S10OD020056.

The sequences presented in this article have been submitted to the Gene Expression Omnibus (https://www.ncbi.nlm.nih.gov/geo/query/acc.cgi?acc=GSE106420) under accession number GSE106420.

Address correspondence and reprint requests to Prof. Donna L. Farber, Columbia Center for Translational Immunology, Columbia University Medical Center, 650 West 168th Street, New York, NY 10032. E-mail address: df2396@cumc.columbia.edu

The online version of this article contains supplemental material.

Abbreviations used in this article: BM, bone marrow; CyTOF, cytometry by time of flight; DE, differentially expressed; LN, lymph node; PCA, principal component analysis; RNA-seq, RNA sequencing; TCF-1, T cell factor-1; TCM, central memory T; TEM, effector memory T; TEMRA, terminally differentiated effector T; Tfh, T follicular helper; TRM, tissue-resident memory T cell; *t*-SNE, *t*-distributed stochastic neighbor embedding.

from those in mouse tissues because of their longevity and/or increased exposure to diverse Ags encountered over human life.

T cell differentiation to effector and memory cell fates is regulated by key transcription factors (8). T cell factor-1 (TCF-1) is essential for memory T cell formation and maintenance in the periphery through regulation of pathways for survival and quiescence (9, 10), whereas T-bet promotes effector over memory T cell generation (11). In mice, differential expression of TCF-1 by memory T cells can influence their function and localization. In mouse models of chronic viral infection, several groups identified a TCF-1$^+$ subset of memory CD8$^+$ T cells to be the responding population mediating viral clearance following anti–PD-1 therapy (12, 13). This TCF-1$^+$ memory subset was absent from peripheral blood and only detected in lymphoid sites (12–16). For human T cells, the role of specific transcription factors in the differentiation, maintenance, and localization of effector and memory T cells has not been defined.

In this study, we used our unique tissue resource from which we obtain blood and multiple lymphoid and mucosal tissues from individual organ donors of all ages (6, 17, 18) to investigate how T cells in lymphoid sites are transcriptionally and functionally related to those in blood and peripheral sites. By studying T cells across multiple tissues within and between individuals, we demonstrate in this study that memory CD8$^+$ T cells are maintained in human LN in an organ-specific manner throughout the human lifespan. Notably, LN memory CD8$^+$ T cells maintain expression of transcription factors TCF-1 and LEF-1 (associated with self-renewal) and exhibit distinct transcriptional and protein expression signatures involved in T follicular helper (Tfh) cell differentiation (with downregulation of effector function and inflammatory signals) compared with memory T cells in blood and other lymphoid (spleen, BM) and peripheral (e.g., lungs) sites. LN memory CD8$^+$ T cells also exhibit higher proliferative capacity and increased TCR clonal diversity compared with memory T cells in other sites. Together these findings establish human LN as reservoirs for maintenance of high-potential memory T cells and LN memory CD8$^+$ T cells as novel targets for immune modulation and adoptive immunotherapies.

Materials and Methods

Acquisition of human tissue

Human tissues were obtained from deceased (brain-dead) organ donors at the time of organ acquisition for lifesaving clinical transplantation (6, 17, 18) through an approved protocol with LiveOnNY, the organ procurement organization for the New York metropolitan area. Donors were free of chronic disease and cancer and negative for hepatitis B, hepatitis C, and HIV. The study does not qualify as human subjects research, as confirmed by the Columbia University Institutional Review Board, because samples were obtained from deceased individuals. See Supplemental Table I for donors used in this study.

Isolation of lymphocytes from human tissues

Tissue samples were maintained in cold saline and brought to the laboratory within 2–4 h of procurement. Mononuclear cells were isolated from blood and BM with Lymphocyte Separation Medium (Corning) and RBC lysis using ACK lysing buffer (Lonza). LN (lung draining, mesenteric, and iliac), spleen, and lung were digested as previously described (6, 18); the resulting suspension was passed through a tissue sieve (10–150 mesh size), and dead cells and debris were removed via centrifugation through 30% Percoll (GE Healthcare Life Sciences, Pittsburgh, PA).

Flow cytometry and sorting

For surface staining, cells were incubated with Abs (see Supplemental Table II for a list) for 30 min at 4°C in the dark along with DAPI (BioLegend). For intracellular staining, cells were incubated in fixation/permeabilization buffer (eBioscience) and stained with Abs for 60 min at 20–25°C. Cells were acquired on a BD LSRII flow cytometer or sorted with a BD Influx cell sorter (BD Biosciences) and analyzed using FlowJo (Tree Star, Ashland, OR).

Whole-transcriptome profiling by RNA sequencing

Total RNA was isolated from sorted cells (gating strategy in Supplemental Fig. 1) using AllPrep DNA/RNA Mini Kit (QIAGEN, Valencia, CA) and quantitated using the Bioanalyzer (Agilent). A library was prepared using a poly-A pull-down and Illumina TruSeq RNA Library Prep Kit and sequenced using Illumina HiSeq 2000. Sequencing data are available online through Gene Expression Omnibus at accession no. GSE106420. Analysis was done using R programming language package DESeq2 (19). For multidimensional scaling analysis, we used the *cmdscale* and *dist* functions in R. For heatmaps, *Z*-score of rlog-normalized values were plotted using *pheatmap*. For analysis in Fig. 2, CD69$^+$ and CD69$^-$ RNA sequencing (RNA-seq) samples were analyzed together by calculating the average of the counts for each gene, normalized using DeSeq2, to examine all CD45RO$^+$ cells and analyzed separately in Supplemental Fig. 1.

Cytometry by time of flight sample preparation and analysis

Cryopreserved cell suspensions were thawed and labeled with Rh103 intercalator as a viability marker. Cells from each tissue were barcoded using CD45 Abs conjugated with monoisotopic cisplatin, pooled, and stained with a panel of Abs (see Supplemental Table II). Samples were then incubated in 0.125-nM Cell-ID Intercalator-Ir and acquired on a CyTOF2 (Fluidigm). The data were deconvolved for each tissue by Boolean gating on CD45 barcodes, leaving DNA$^+$CD45$^+$Rh103$^-$ singlets for analysis. Data were visualized using principal component analysis (PCA) and viSNE (19) and implemented using FCS Express v6 (De Novo Software, CA). For heatmaps, samples were clustered by unsupervised hierarchical clustering with the R function *hclust*.

T cell proliferation assays

Memory CD8$^+$ T cells from BM, LN, spleen, or lung tissues were sorted (Supplemental Fig. 1) and stained with Proliferation Dye eFluor 450 (eBioscience). Cells were plated (5 × 105 cells/ml) in medium (RPMI 1640, 10% FBS, 1 mM sodium pyruvate, 100 U/ml penicillin, 100 μg/ml streptomycin, 2 mM L-glutamine, and 100 μM 2-ME) with Human CD3/CD28 T Cell Activator (STEMCELL Technologies) and analyzed 4–5 d later by flow cytometry. In some cases, whole mononuclear cells from blood, BM, or LN were cultured with 0.3 μg/ml human CMV pp65 peptide mixture (JPT Peptide Technologies). IL-2 (100 U/ml) was added on day 2, and cells were analyzed at day 8 or 9 after stimulation. Cells were stained with HLA multimer reagents containing epitopes of CMV (CMV-multimer) (Supplemental Table II) as previously described (20).

Human TCR sequencing and analysis

DNA was extracted from cells using the Gentra Puregene Tissue Kit (QIAGEN). TCR-Vβ sequences were amplified from the indicated DNA quantities (Supplemental Table III) with specific primers as published previously (21). Amplicons were purified using the AMPure XP system (Beckman Coulter, Indianapolis, IN); libraries were generated using the QIAGEN Multiplex PCR Kit and sequenced using Illumina MiSeq. Raw sequence data (FASTQ files) were filtered as previously described (22), and clone assemblies were processed by MiXCR (v2.1) (23). Clonality was measured for all TCR clones by normalizing the entropy values of each sample to the number of unique TCR sequences, resulting in a value ranging from 0 (most diverse) to 1 (least diverse). Given a clonotype x, the frequency of that clonotype, denoted as $p(x)$, was used to calculate Shannon entropy (H) of a TCR repertoire X as follows:

$$H(X) = -\sum_{x \in X} p(x) log_2\ p(x)$$

Normalized entropy (H_{norm}) is calculated to control for set size, where L is the total number of unique clonotypes in the sample, as follows:

$$H_{norm}(X) = \frac{H(X)}{-log_2\ \frac{1}{L}}$$

Next, clonality is calculated as follows: Clonality (X) = 1 − $H_{norm}(X)$ (24). For clonality and diversity analysis, the same input T cell DNA was used and calculated using different orders (25, 26).

Statistical analysis

Bar graphs depict the mean ± SEM or ± SD as indicated. Statistical analyses were performed with Prism 6.0 (GraphPad Software). Paired

and nonpaired *t* tests (two tailed) were used as indicated. The *p* values ≤0.05 were considered significant; *p* values >0.05 were nonsignificant.

Results

Human memory T cells exhibit increased TCF-1 expression in LN compared with other tissues

Human T cells can be subdivided into major subsets based on CD45RA and CCR7 expression: naive ($CD45RA^+CCR7^+$), central memory T (TCM) ($CD45RA^-CCR7^+$), effector memory T (TEM) ($CD45RA^-CCR7^-$), and terminally differentiated effector T (TEMRA) cells ($CD45RA^+CCR7^-$) (6). For $CD8^+$ T cells, TEM phenotype cells are the predominant memory T cell subset in blood and diverse tissue sites, with low frequencies of TCM-phenotype cells (6), as shown in this study in BM, spleen, lung, and LN (Fig. 1A). We examined whether $CD8^+$ TEM cells exhibited tissue-specific variations in expression of TCF-1, a transcription factor associated with stem cell–like function (9). In all donors, TCF-1 expression by $CD8^+$ TEM in LN was significantly higher than that found in $CD8^+$ TEM derived from blood, BM, spleen, and lung (Fig. 1B). TCF-$1^{hi}CD8^+$ TEM cells were observed in LN draining different anatomical sites (lungs, intestines, groin; Fig. 1B) and across all ages (9–76 y; Fig. 1C). Moreover, TCF-1 expression was comparably high within $CD69^+$ and $CD69^-$ subsets of LN memory T cells (Supplemental Fig. 1), delineating circulating and tissue-resident memory populations (4). These results suggest that increased TCF-1 expression is an organ-specific (rather than subset-specific) feature of memory $CD8^+$ T cells within LN.

Human LN memory T cells exhibit a distinct phenotype and transcriptional profile

We used whole-transcriptome profiling by RNA-seq to investigate whether increased TCF-1 expression by LN memory $CD8^+$ T cells indicated a distinct transcriptional program compared with memory $CD8^+$ T cells in blood and other lymphoid sites. We initially analyzed differential gene expression between memory $CD8^+$ T cells in LN and BM of three individuals (see sorting strategy; Supplemental Fig. 1), identifying over 2000 differentially expressed (DE) genes conserved between individuals, many of which included markers associated with T cell differentiation by pathway analysis (Supplemental Table IV). In particular, LN memory $CD8^+$ T cells had increased expression of transcripts associated with self-renewal (*LEF1*, *TCF7*), Tfh cell differentiation (27–29) (*BCL6*, *CXCR5*, *CXCR4*, *CCR7*), costimulation (*CD28*, *ICOS*), and reduced expression of effector transcripts (*GZMA*, *PRF1*) (Fig. 2A). Genes involved in Wnt signaling (*WNT10A*, *CD44*, *SOX13*) and cell cycle control (*CDKN1A*, *CDKN2C*) were also DE in LN compared with BM memory $CD8^+$ T cells (Fig. 2A). Analysis of protein expression confirmed increased CXCR4 and LEF-1 expression and decreased expression of perforin and T-bet in human LN compared with BM $CD8^+$memory T cells (Fig. 2B).

We further compared the transcriptional profile of LN memory $CD8^+$ T cells to that in blood and other tissues, including spleen and lungs, for which we previously obtained RNA-seq profiles (4). Based on the DE genes derived from Fig. 2A, the transcriptional profile of LN memory $CD8^+$ T cells clustered together by PCA, distinct from that of memory $CD8^+$ T cells in blood, BM, spleen, and lung for all donors analyzed (Fig. 2C). Through paired analysis of gene expression between LN and these other sites, we identified a gene signature of 348 upregulated and 349 downregulated genes in LN memory $CD8^+$ T cells compared with the corresponding subset in blood, spleen, or BM (Supplemental Table V). Notably, genes involved in Tfh cell differentiation (30) were upregulated in LN (*IL21R*, *LEF1*, and *ICOS*), and genes involved in homing and cytotoxic function were downregulated (*S1PR5*, *FCER1G*, *GRMH*, and *NKG7*) in LN compared with blood, spleen, and BM memory $CD8^+$ T cells (Fig. 2D).

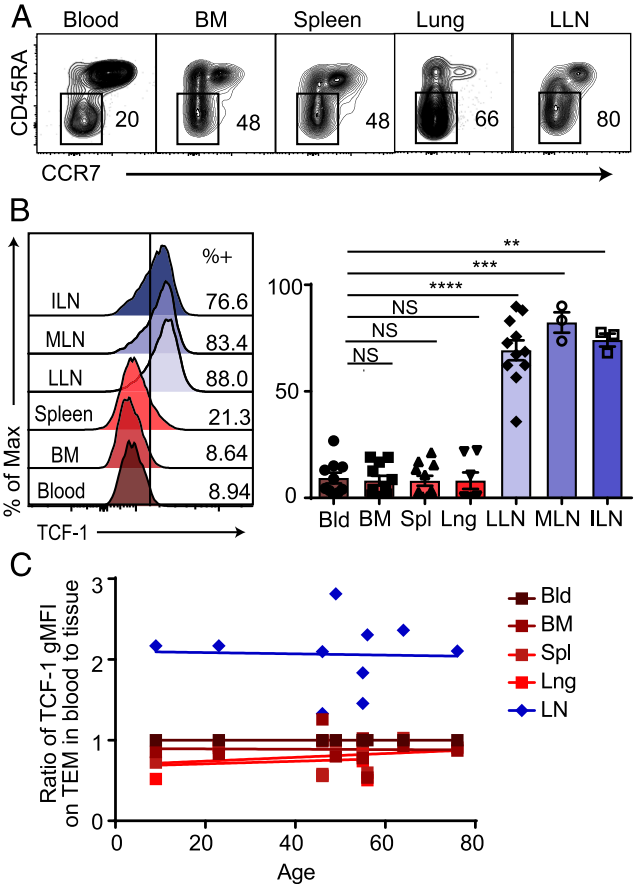

FIGURE 1. Tissue-specific lifelong maintenance of TCF-1 expression by human LN memory $CD8^+$ T cells. (**A**) $CD3^+CD8^+$ T cell subset composition showing frequencies of TEM ($CD45RA^-CCR7^-$) in blood and tissues from a representative individual (D251; see Supplemental Table I for donor information). (**B**) TCF-1 expression is restricted to LN TEM cells. Left, TCF-1 expression by $CD8^+$ TEM cells in representative histograms from one donor (D334). Right, Compiled frequencies from multiple donors ($n = 11$). (**C**) LN-specific TCF-1 expression is maintained with age. Ratio of TCF-1 geometric mean fluorescence intensity (gMFI) by $CD8^+$ TEM in tissues to that in blood. Error bars indicate SEM. NS by two-tailed *t* test. $^{**}p < 0.01$, $^{***}p < 0.001$, $^{****}p < 0.0001$. ILN, iliac-draining LN; LLN, lung-draining LN; Lng, lung; MLN, mesenteric-draining LN; Spl, spleen.

To dissect mechanisms for the distinct gene expression profile of LN memory $CD8^+$ T cells, we analyzed pathways and upstream regulators. Pathway analysis showed conserved upregulated (Tfh cell, cell cycle, stem cell) and downregulated (T cell activation, signaling, and inflammation) pathways in memory $CD8^+$ T cells from LN compared with BM, spleen, and blood (Supplemental Table IV). Potential upstream regulators of LN memory cells were associated with cell survival and growth factors (i.e., FOXO1, NOTCH1, and EGFR), whereas molecules involving IFN signaling and type I IFN responses (i.e., STAT1, IFNA2, and IFNB1) were enriched in memory $CD8^+$ T cells derived from blood, BM, and spleen (Table I). Therefore, LN memory $CD8^+$ T cells exhibit a distinct transcriptional program marked by quiescence and survival, whereas memory $CD8^+$ T cells in BM, spleen, and blood exhibit cellular signatures associated with effector function and inflammatory signals.

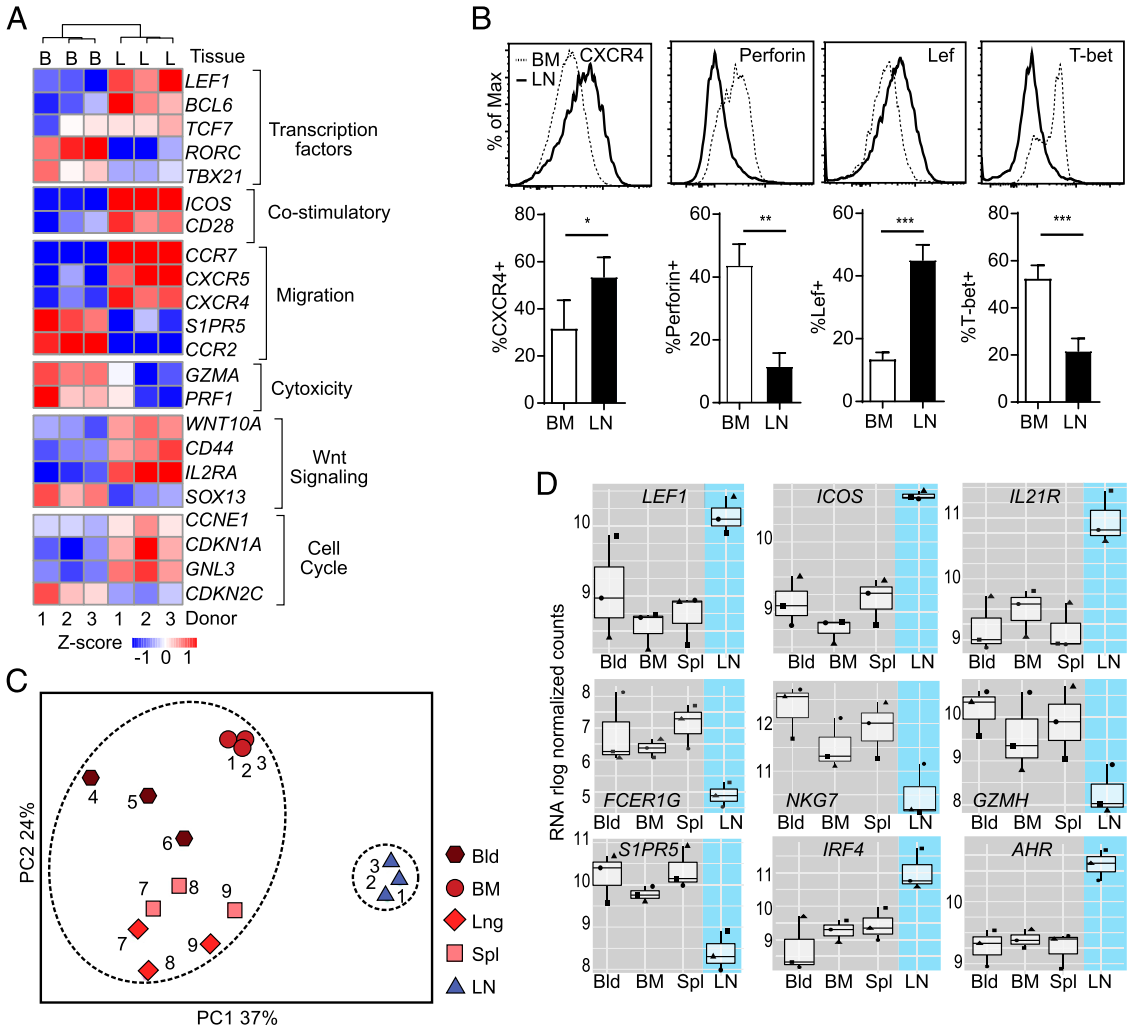

FIGURE 2. Human LN memory CD8$^+$ T cells are phenotypically and transcriptionally distinct from peripheral blood and lymphoid-derived T cells. (**A**) Heatmap of RNA-seq data showing relative expression of key genes DE between BM and LN (B and L, respectively) CD8$^+$ TEM cells from three donors. (**B**) Protein expression of markers identified in (A), shown as histograms from one donor (top, from left to right: D259, D304, D227, D273; Supplemental Table I) and compiled (bottom: CXCR4 [$n = 8$], perforin [$n = 5$], Lef [$n = 7$], T-bet [$n = 13$]). (**C**) PCA of transcriptional profiles of CD8$^+$ TEM cells from blood (Bld), BM, lung (Lng), spleen (Spl), and LN from nine individuals (1–9) based on the 2521 DE genes between LN and BM memory CD8$^+$ T cells. (**D**) Relative transcript expression of indicated genes among CD8$^+$ TEM cells from blood and tissue sites of nine individuals in (C). Error bars indicate SEM. $*p < 0.05$, $**p < 0.01$, $***p < 0.001$ by two-tailed t test.

Human LN memory T cells are transcriptionally similar to murine TCF-1^{hi} CD8$^+$ T cells that respond to checkpoint blockade

We investigated whether the distinct transcriptional profile of LN memory CD8$^+$ T cells was due to enrichment of a specific subset, such as TCM or TRM within the LN, or was organ specific. The LN-specific memory CD8$^+$ T cell profile identified in Fig. 2 was not significantly similar to that previously defined for blood CD8$^+$ TCM cells (18 shared genes of 785 TCM-associated genes) (31, 32). Moreover, the LN-specific gene signature identified in Fig. 2 was conserved within both CD69$^+$ (TRM phenotype) and CD69$^-$ (circulating) memory subsets (Supplemental Fig. 1). Therefore, the distinct transcriptional profile of human LN memory CD8$^+$ T cells is not attributed to an enrichment of TCM or TRM subsets.

We then considered whether the Tfh cell–like profile of human LN memory CD8$^+$ T cells could be similar to a recently defined Tfh cell–like PD-1^{hi}TCF-1^{hi}CXCR5$^+$ memory CD8$^+$ T cell subset identified in mouse chronic infection models that mediated viral clearance and proliferated in response to anti–PD-1 checkpoint blockade (12–16). By gene set enrichment analysis (33), we found significant homology in the complement of up- and downregulated genes between the human LN-specific gene signature and the gene signature of mouse TCF-1$^+$ memory versus TCF-1$^-$ CD8$^+$ T cells from two independent studies (12, 13) (Fig. 3A). Key genes shared between mouse and human subsets include those encoding transcriptional regulators (*ID3*, *TCF7*, *BCL6*), homing molecules (*CXCR5*, *CCR7*), cytokines, effector molecules (*GZMB*), and cell cycle regulators (*CDCA3*, *CDC8*) (Fig. 3B). Human LN memory CD8$^+$ T cells therefore exhibit an organ-specific transcriptional profile similar to a T cell subset that maintains and restores immune responses to persistent pathogens in mice.

Defining an organ-specific protein signature of LN memory CD8$^+$ T cells by cytometry by time of flight

We used cytometry by time of flight (CyTOF) to define a protein expression signature of LN memory CD8$^+$ T cells relative to other sites based on the transcriptional profile identified above. We analyzed CD8$^+$ T cells from four tissue sites (LN, BM, spleen, and lungs) of three individual donors using a 35-marker CyTOF panel, including markers of T cell differentiation, function, and proliferation

Table I. Type 1 IFN pathways are inhibited in LN memory CD8$^+$ T cells compared to blood and other sites

Upstream Regulators	Molecule Type	Direction in LN	Z-Score
Ifnar	Group	Inhibited	−3.27
IFN-α/β	Group	Inhibited	−2.30
IFNA2	Cytokine	Inhibited	−2.74
IFNB1	Cytokine	Inhibited	−2.65
STAT1	Transcription regulator	Inhibited	−2.67
STAT3	Transcription regulator	Activated	1.48
FOXO1	Transcription regulator	Activated	0.72
NOTCH1	Transcription regulator	Activated	3.16
Vegf	Group	Activated	3.47
HGF	Growth factor	Activated	3.11
EGFR	Kinase	Activated	3.48

Upstream regulators were identified as significantly enriched (p value <0.05). Z-score indicates predicted direction of regulator activity in memory CD8$^+$ T cells from LN (inhibited or activated) compared with blood, BM, and spleen. Results were obtained from Ingenuity Pathway Analysis software (QIAGEN) by comparison of memory T cells isolated from different tissues (LN versus BM, LN versus blood, and LN versus spleen).

as well as transcription factors (see Supplemental Table II). Subset- and tissue-specific variations within and between donors were assessed using t-distributed stochastic neighbor embedding (t-SNE) analysis, a dimensionality reduction algorithm (34), on combined data for all tissues and donors. A total of 23 markers were used to generate the t-SNE plot, with the contribution of each individual marker and its expression density shown in Supplemental Fig. 2. The concatenated analysis reveals that TCF-1 and CD28 segregate on distinct regions of the t-SNE plots relative to T-bet and granzyme B expression (Fig. 4A), which correspond to naive (CD45RA$^+$CCR7$^+$) and TEMRA cells (CD45RA$^+$CCR7$^-$), respectively (Fig. 4B). By contrast, CD8$^+$ TEM cells (memory, CD45RA$^-$CCR7$^-$) cluster on broader regions of the t-SNE plot, with the higher-density clusters on regions distinct from naive and TEMRA cells, indicating heterogeneity of memory CD8$^+$ T cells.

We dissected the heterogeneity of CD8$^+$ TEM cells by tissue site and individual. For both donors shown, CD8$^+$ TEM in BM and lung were most similar to each other and contained regions that overlapped with regions denoted by TEM and TEMRA cells and with splenic CD8$^+$ TEM cells (Fig. 4B, 4C). In LN, CD8$^+$ TEM occupied a distinct region of the t-SNE, showing overlap with CD8$^+$ TEM from spleen but not from BM and lung (Fig. 4C). We further stratified memory CD8$^+$ T cells by CD69 expression to delineate putative tissue residency (4). The t-SNE profile of CD69$^+$ TEM cells was similar in the four tissue sites (LN, spleen, BM, and lung) (Fig. 4D), consistent with the finding that CD69$^+$ tissue memory T cells exhibit a core signature of TRM (4). However, the t-SNE profile of CD69$^-$ TEM was distinct in LN and similar in spleen, lung, and BM (Fig. 4D), and the LN CD69$^-$ TEM cell profile was not observed in blood (Fig. 4E). Interestingly the LN CD69$^-$ TEM cell profile was similar to LN CD69$^+$ TEM cells, whereas in other sites, these two subsets were distinct (Fig. 4D). Together, these findings indicate that LN memory CD8$^+$ T cells exhibit a protein expression signature that is organ specific and not found in circulation or other tissues.

LN memory CD8$^+$ T cells exhibit a differentiation signature with similarities to both naive and memory T cells

To identify which markers were driving the LN-specific signature identified above, we used clustering analysis, which revealed that LN memory CD8$^+$ T cells express a unique combination of markers, including those shared with naive T cells (cluster I and IV) and others with memory CD8$^+$ T cells in blood and other sites

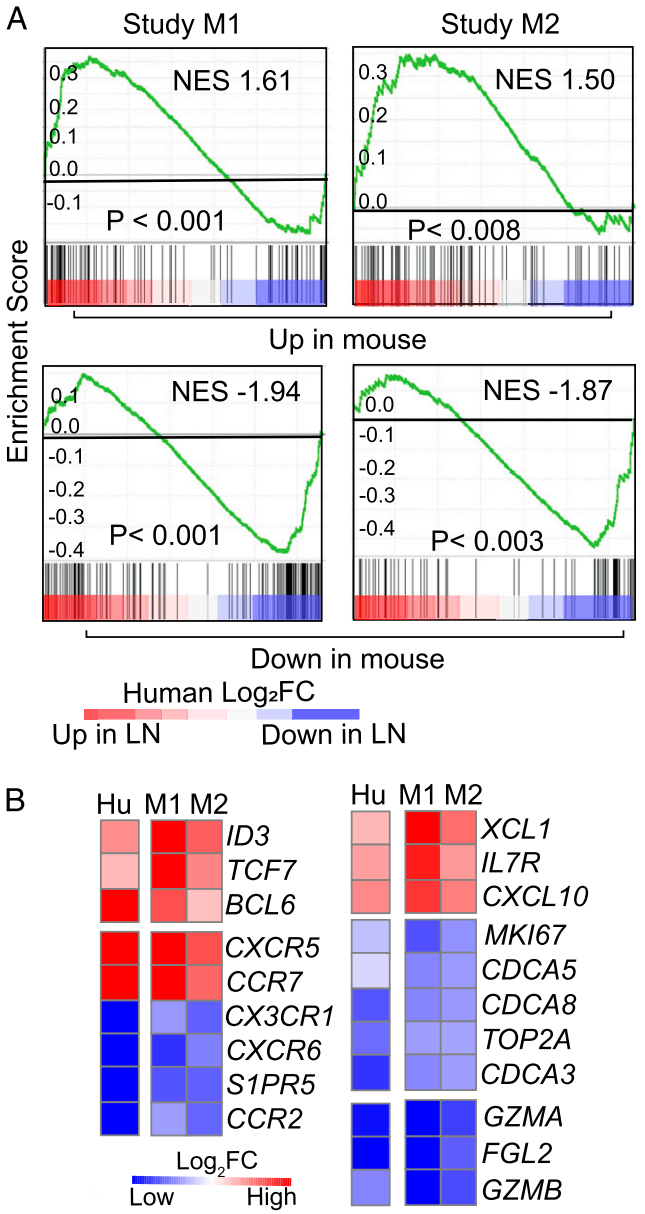

FIGURE 3. Human LN memory CD8$^+$ T cells exhibit similarity to murine stem cell–like T cells. (**A**) Comparison of mouse stem cell–like T cell transcriptome to human LN memory T cells by gene set enrichment analysis based on human DE genes from Fig. 2C compared with ranked lists of up- or downregulated genes between TCF-1$^+$ versus TCF-1$^-$ cells from two mouse studies (M1, M2) (12, 13). From the published studies, we ranked the top 500 DE genes from microarray or the significantly DE genes from RNA-seq (false discovery rate ≤ 0.05, |fold change| ≥ 1). (**B**) Heatmap showing relative expression fold change (FC) of genes from human LN (Hu) versus BM CD8$^+$ TEM cells compared with mouse subsets M1 and M2. NES, normalized enrichment score.

(cluster II and III) (Fig. 5A). Integrating the CyTOF data from multiple tissues and donors by multidimensional scaling and k-means clustering analysis further shows that LN memory CD8$^+$ T cells have a protein expression signature that is distinct from naive and memory T cells in other sites (Fig. 5B). PCA based on the protein expression data further reveals that LN TEM cells are more similar to naive T cells, whereas tissue TEM are more similar to TEMRA cells, which represent the most differentiated subset (Fig. 5C). These analyses show that LN memory CD8$^+$ T cells exhibit a less differentiated profile when compared with memory T cells in blood and other lymphoid and mucosal sites.

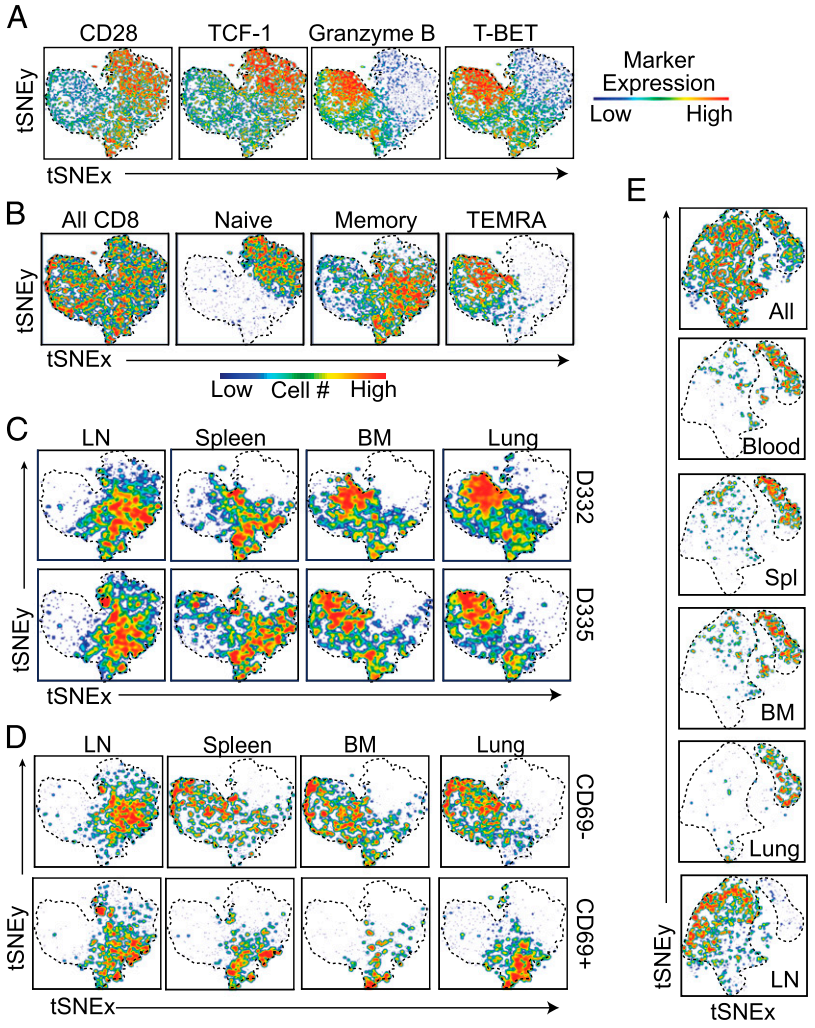

FIGURE 4. Human LN memory CD8$^+$ T cells exhibit a protein signature distinct from blood and other tissue sites. T cells from LN, BM, spleen, lung, and blood were stained with a 35-color panel (Supplemental Table II) and analyzed by CyTOF. (**A**) Expression of indicated markers on *t*-SNE plots of total CD8$^+$ T cells from BM, spleen, LN, and lung of three individuals (D332, D333, and D335; Supplemental Table I) based on 20 markers (CD57, CD28, perforin, CD127, PD-1, ICOS, CD27, CCR5, TCF-1, CXCR5, 41BB, CD25, T-bet, CD38, CD95, LAG3, CXCR4, HLA-DR, TIGIT, and granzyme B; Supplemental Fig. 2) (**B**) Density plots as in (A) gated on naive (CD45RA$^+$CCR7$^+$), memory (CD45RA$^-$CCR7$^-$), and TEMRA (CD45RA$^+$CCR7$^-$) CD8$^+$ T cells. (**C**) Density plots as in (A) showing CD8$^+$ TEM (donor 332 [top row] and donor 335 [bottom row]). (**D**) Memory T cells from indicated tissues, gated on CD69$^-$ (top) or CD69$^+$ (bottom) subsets. (**E**) Comparison of TEM CD69$^-$ from blood and indicated tissues of one individual (D342) by *t*-SNE density plots based on markers in (A) minus TCF-1.

Enhanced proliferative capacity of LN memory CD8$^+$ T cells

Functionally, TCF-1 expression is associated with a higher proliferative capacity to TCR-driven stimulation (35). When stimulated with anti-CD3/anti-CD28 Abs, LN memory CD8$^+$ T cells exhibited greater proliferation compared with counterparts in BM, spleen, and lung (Fig. 6A, 6C). After CD3/CD28 stimulation, LN CD8$^+$ TEM cell counts were between 98 and 106-fold higher than BM. T-bet expression was also increased to a greater extent in LN CD8$^+$ TEM cells following stimulation compared with other sites, both in the level of expression and the fold change increase following activation (Fig. 6B, 6D). Increased proliferation by LN memory CD8$^+$ T cells was also observed with Ag stimulation, as CMV-specific CD8$^+$ TEM cells from LN proliferated to a greater extent in response to CMV peptide Ags compared with BM CD8$^+$ TEM cells (Supplemental Fig. 1). Together, these results demonstrate that LN memory CD8$^+$ T cells have a higher capacity for proliferation and differentiation compared with memory CD8$^+$ T cells in other sites.

Increased TCR clonal diversity among LN compared with BM memory T cells

The results above indicate that memory CD8$^+$ T cells in LN exhibit a more quiescent state compared with other sites, including the BM, which is a known reservoir for memory T cells of multiple specificities (36). To assess whether there was differential maintenance of clonal populations between LN and BM memory T cells, we performed sequencing of the TCR CDR3β V regions of memory CD8$^+$ T cells isolated from multiple donors (see *Materials and Methods* and Supplemental Fig. 1). We found more different V region sequences from comparable numbers of LN compared with BM memory CD8$^+$ T cells for all donors (Supplemental Table III). Importantly, BM memory CD8$^+$ T cells consistently had higher clonality compared with LN memory CD8$^+$ T cells (Fig. 7A). Conversely, an increase in TCR diversity was observed for LN compared with BM memory CD8$^+$ T cells for all donors, even when controlling for clone size (Fig. 7B). Together, these results show that memory CD8$^+$ T cells in LN represent a more clonally diverse population than is maintained in blood and other tissue sites, consistent with our findings that LN memory CD8$^+$ T cells are maintained in a quiescent state.

Discussion

The majority of human T cells are found in lymphoid sites, although their function and relationship to blood T cells has been challenging to assess using conventional sampling. By examination of T cell subsets in human blood and tissue sites of individual organ donors, we demonstrate in this study that LN memory CD8$^+$ T cells exhibit organ-specific profiles not found in blood or other lymphoid (BM, spleen) or mucosal tissues. Specifically, LN memory T cells exhibit transcriptional and phenotypic signatures associated with quiescence, high proliferative capacity, and enhanced TCR diversity compared with memory T cells in blood and other tissues that are enriched for effector function and

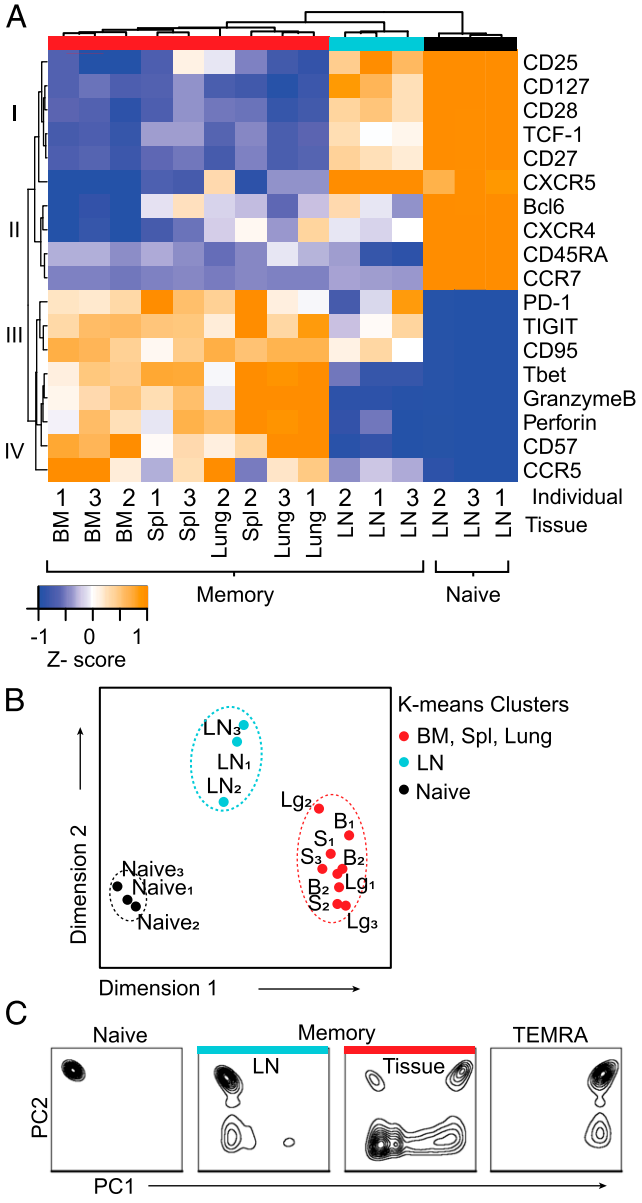

FIGURE 5. LN memory CD8$^+$ T cells exhibit a differentiation profile with features of both naive and memory T cells. (**A**) T cells from LN, BM, spleen, and lung were stained with a 35-color panel (Supplemental Table II) and analyzed by CyTOF. Heatmap showing relative expression of indicated proteins by naive and TEM CD69$^-$ populations in tissues of three donors from Fig. 4. (**B**) Multidimensional scaling (MDS) plot of T cell subsets by *k*-means clustering. (**C**) PCA of indicated T cell subsets, including total memory and TEMRA from LN (blue) and BM, spleen, and lung (red) from donors, as in (A).

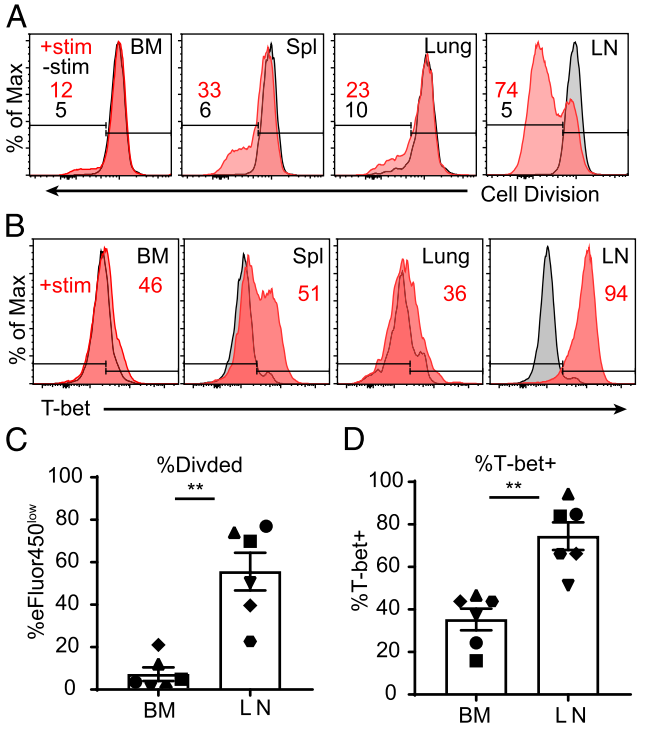

FIGURE 6. Human LN memory CD8$^+$ T cells exhibit enhanced proliferation and effector phenotype in response to TCR stimulation compared with other lymphoid and mucosal sites. (**A**) Proliferation of CD8$^+$ TEM cells to anti-CD3/CD28 stimulation shown as percentage of eFluor 450–negative cells (divided cells) (red) compared with unstimulated cells (black) from a representative individual (D377) (**B**) Expression of transcription factor T-bet shown as the percentage positive on stimulated T cells from indicated tissue sites from a representative individual (D377). (**C**) Data from (A) compiled from six individuals by percentage divided (percentage eFluor 450^{low}) and (**D**) data from (B) compiled from six individuals by the percentage positive for T-bet expression in stimulated cells. Error bars indicate SEM. $^{**}p < 0.01$ by two-tailed *t* test.

inflammatory signatures. Our findings reveal that human LN serve as reservoirs for long-term maintenance of functional T cell responses and an important source for targeting in vaccines and immunotherapies.

We demonstrate in this study that memory T cells derived from LN maintain expression of the TCF-1 transcription factor associated with quiescence over decades of adult life. These results suggest differential priming of memory CD8$^+$ T cells that persist in LN compared with those that migrate and take up residence in other tissue sites. Recent studies in a mouse model of influenza infection showed differential TCF-1 expression by T cells primed in different LN sites: in the lung-draining LN there was rapid downregulation of TCF-1 expression, whereas TCF-1 expression was maintained by T cells primed to proliferate in a nondraining LN site, with reduced Ag and inflammatory signals (37). We propose that memory T cells in LN do not receive the full differentiation signals to promote LN egress and migration to the tissue site of infection and therefore get retained and maintained with increased TCF-1 expression.

LN memory CD8$^+$ T cells exhibit a transcriptional and protein signature with homology to a mouse memory CD8$^+$ T cell subset generated during chronic virus infection that maintained functional capacity, proliferated, and mediated viral clearance in response to anti–PD-1 therapy (12–16). Whether human LN memory T cells provide similar roles in controlling chronic viral infection remains to be established; however, we previously showed that certain individuals with persistent CMV infection maintained CMV-specific CD8$^+$ T cells exclusively in LN but not in circulation or other tissue sites (20). Additionally, HIV-specific resident memory CD8$^+$ T cells were recently characterized in human LN (38). These results suggest that human LN can maintain reservoirs of antiviral memory T cells. Moreover, the maintenance of higher TCR diversity among LN memory CD8$^+$ T cells suggests a unique role in maintaining functional T cell immunity over the lifespan, with the potential to respond to different pathogens, which is of potential importance for targeting in vaccines.

The mechanisms by which human LN maintain this distinct TCF-1^{hi} memory subset are not known, although there is evidence that protection from IFN signaling may play a role. Transcriptionally,

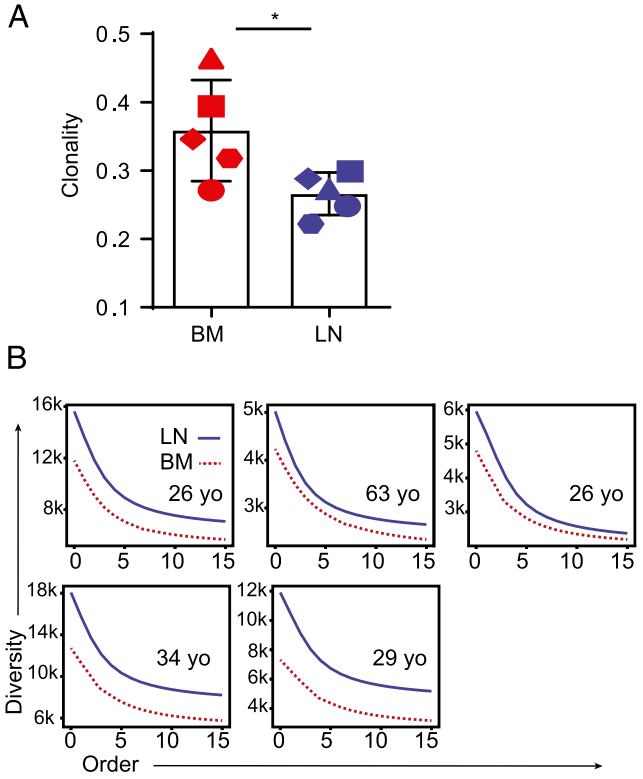

FIGURE 7. LN memory CD8$^+$ T cells maintain high TCR diversity. (**A**) Clonality of TCR CDR3β sequences for CD8$^+$ TEM in BM and LN among five individuals. (**B**) Diversity of TCR sequences at different orders is shown for CD8$^+$ TEM cells from BM (dotted red) and LN (solid blue) among five individuals. At order zero, diversity is the total number of clones (richness). As order increases, the most abundant clones are given more weight. Error bars indicate SEM. *$p < 0.05$ by two-tailed t test.

LN memory CD8$^+$ T cells exhibited downregulation of pathways involved in type 1 IFN signaling, which were correspondingly upregulated in blood, BM, and spleen memory T cells. Furthermore, inhibiting type 1 IFN signaling during viral infection in mice led to higher accumulation of TCF-1$^+$ T cells in a T cell–intrinsic manner (16). Compared with mucosal and barrier sites, which are constantly exposed to diverse microbial Ags, human LN are likely exposed to lower levels of inflammation and Ags and thus provide protective niches for long-term maintenance of functional memory T cells.

Our results suggest that LN memory CD8$^+$ T cells are a potentially important source of functional T cells to target in immunotherapies for antitumor immunity. Given their homology to the mouse subset, LN memory T cells could analogously provide a source of highly proliferative T cells to respond to anti–PD-1 therapy. Memory T cells in LN- draining sites of tumors could therefore be targeted for expansion of highly functional T cells to infiltrate the tumor site. Isolation of high-potential memory subsets from blood has been a matter of considerable investigation in the field of adoptive cellular therapy to optimize the persistence of expanded, differentiated cell populations (39) and to serve as a source of cells for transfection of targeted molecules for therapies in hematopoietic malignancies (40). We propose that LN could be a more optimal source for memory T cells for adoptive immunotherapies compared with blood based on their increased proliferative potential and capacity to respond to diverse Ags.

In summary, our results provide evidence for long-term persistence of a distinct, organ-specific T cell subset in human LN. These findings demonstrate that tissue localization is a major determinant for human T cell differentiation, with LN providing long-term reservoirs for quiescent immunological memories important for targeting in vaccines and immunotherapies.

Acknowledgments

We thank the generosity of the donor families and the efforts of the Live-OnNY transplant coordinators and staff for making this study possible.

Disclosures

The authors have no financial conflicts of interest.

References

1. Farber, D. L., N. A. Yudanin, and N. P. Restifo. 2014. Human memory T cells: generation, compartmentalization and homeostasis. *Nat. Rev. Immunol.* 14: 24–35.
2. Sallusto, F., J. Geginat, and A. Lanzavecchia. 2004. Central memory and effector memory T cell subsets: function, generation, and maintenance. *Annu. Rev. Immunol.* 22: 745–763.
3. Ganusov, V. V., and R. J. De Boer. 2007. Do most lymphocytes in humans really reside in the gut? *Trends Immunol.* 28: 514–518.
4. Kumar, B. V., W. Ma, M. Miron, T. Granot, R. S. Guyer, D. J. Carpenter, T. Senda, X. Sun, S. H. Ho, H. Lerner, et al. 2017. Human tissue-resident memory T cells are defined by core transcriptional and functional signatures in lymphoid and mucosal sites. *Cell Rep.* 20: 2921–2934.
5. Thome, J. J., and D. L. Farber. 2015. Emerging concepts in tissue-resident T cells: lessons from humans. *Trends Immunol.* 36: 428–435.
6. Thome, J. J. C., N. Yudanin, Y. Ohmura, M. Kubota, B. Grinshpun, T. Sathaliyawala, T. Kato, H. Lerner, Y. Shen, and D. L. Farber. 2014. Spatial map of human T cell compartmentalization and maintenance over decades of life. *Cell* 159: 814–828.
7. Teijaro, J. R., D. Turner, Q. Pham, E. J. Wherry, L. Lefrançois, and D. L. Farber. 2011. Cutting edge: tissue-retentive lung memory CD4 T cells mediate optimal protection to respiratory virus infection. *J. Immunol.* 187: 5510–5514.
8. Lin, W. W., S. A. Nish, B. Yen, Y. H. Chen, W. C. Adams, R. Kratchmarov, N. J. Rothman, A. Bhandoola, H. H. Xue, and S. L. Reiner. 2016. CD8$^+$ T Lymphocyte self-renewal during effector cell determination. *Cell Rep.* 17: 1773–1782.
9. Zhou, X., S. Yu, D. M. Zhao, J. T. Harty, V. P. Badovinac, and H. H. Xue. 2010. Differentiation and persistence of memory CD8(+) T cells depend on T cell factor 1. *Immunity* 33: 229–240.
10. Jeannet, G., C. Boudousquié, N. Gardiol, J. Kang, J. Huelsken, and W. Held. 2010. Essential role of the Wnt pathway effector Tcf-1 for the establishment of functional CD8 T cell memory. *Proc. Natl. Acad. Sci. USA* 107: 9777–9782.
11. Joshi, N. S., W. Cui, A. Chandele, H. K. Lee, D. R. Urso, J. Hagman, L. Gapin, and S. M. Kaech. 2007. Inflammation directs memory precursor and short-lived effector CD8(+) T cell fates via the graded expression of T-bet transcription factor. *Immunity* 27: 281–295.
12. Utzschneider, D. T., M. Charmoy, V. Chennupati, L. Pousse, D. P. Ferreira, S. Calderon-Copete, M. Danilo, F. Alfei, M. Hofmann, D. Wieland, et al. 2016. T cell factor 1-expressing memory-like CD8(+) T cells sustain the immune response to chronic viral infections. *Immunity* 45: 415–427.
13. Im, S. J., M. Hashimoto, M. Y. Gerner, J. Lee, H. T. Kissick, M. C. Burger, Q. Shan, J. S. Hale, J. Lee, T. H. Nasti, et al. 2016. Defining CD8+ T cells that provide the proliferative burst after PD-1 therapy. *Nature* 537: 417–421.
14. He, R., S. Hou, C. Liu, A. Zhang, Q. Bai, M. Han, Y. Yang, G. Wei, T. Shen, X. Yang, et al. 2016. Follicular CXCR5- expressing CD8(+) T cells curtail chronic viral infection. [Published erratum appears in 2016 *Nature* 540: 470.] *Nature* 537: 412–428.
15. Leong, Y. A., Y. Chen, H. S. Ong, D. Wu, K. Man, C. Deleage, M. Minnich, B. J. Meckiff, Y. Wei, Z. Hou, et al. 2016. CXCR5(+) follicular cytotoxic T cells control viral infection in B cell follicles. *Nat. Immunol.* 17: 1187–1196.
16. Wu, T., Y. Ji, E. A. Moseman, H. C. Xu, M. Manglani, M. Kirby, S. M. Anderson, R. Handon, E. Kenyon, A. Elkahloun, et al. 2016. The TCF1-Bcl6 axis counteracts type I interferon to repress exhaustion and maintain T cell stemness. *Sci. Immunol.* 1: eaai8593.
17. Carpenter, D. J., T. Granot, N. Matsuoka, T. Senda, B. V. Kumar, J. J. C. Thome, C. L. Gordon, M. Miron, J. Weiner, T. Connors, et al. 2018. Human immunology studies using organ donors: impact of clinical variations on immune parameters in tissues and circulation. *Am. J. Transpl.* 18: 74–88.
18. Sathaliyawala, T., M. Kubota, N. Yudanin, D. Turner, P. Camp, J. J. Thome, K. L. Bickham, H. Lerner, M. Goldstein, M. Sykes, et al. 2013. Distribution and compartmentalization of human circulating and tissue-resident memory T cell subsets. *Immunity* 38: 187–197.
19. Love, M. I., W. Huber, and S. Anders. 2014. Moderated estimation of fold change and dispersion for RNA-seq data with DESeq2. *Genome Biol.* 15: 550.
20. Gordon, C. L., M. Miron, J. J. Thome, N. Matsuoka, J. Weiner, M. A. Rak, S. Igarashi, T. Granot, H. Lerner, F. Goodrum, and D. L. Farber. 2017. Tissue reservoirs of antiviral T cell immunity in persistent human CMV infection. *J. Exp. Med.* 214: 651–667.
21. van Dongen, J. J., A. W. Langerak, M. Brüggemann, P. A. Evans, M. Hummel, F. L. Lavender, E. Delabesse, F. Davi, E. Schuuring, R. García-Sanz, et al. 2003. Design and standardization of PCR primers and protocols for detection of clonal immunoglobulin and T-cell receptor gene recombinations in suspect

lymphoproliferations: report of the BIOMED-2 Concerted Action BMH4-CT98-3936. *Leukemia* 17: 2257–2317.
22. Meng, W., B. Zhang, G. W. Schwartz, A. M. Rosenfeld, D. Ren, J. J. C. Thome, D. J. Carpenter, N. Matsuoka, H. Lerner, A. L. Friedman, et al. 2017. An atlas of B-cell clonal distribution in the human body. *Nat. Biotechnol.* 35: 879–884.
23. Bolotin, D. A., S. Poslavsky, I. Mitrophanov, M. Shugay, I. Z. Mamedov, E. V. Putintseva, and D. M. Chudakov. 2015. MiXCR: software for comprehensive adaptive immunity profiling. *Nat. Methods* 12: 380–381.
24. Thome, J. J., B. Grinshpun, B. V. Kumar, M. Kubota, Y. Ohmura, H. Lerner, G. D. Sempowski, Y. Shen, and D. L. Farber. 2016. Longterm maintenance of human naive T cells through *in situ* homeostasis in lymphoid tissue sites. *Sci. Immunol.* 1: eaah6506.
25. Schwartz, G. W., and U. Hershberg. 2013. Conserved variation: identifying patterns of stability and variability in BCR and TCR V genes with different diversity and richness metrics. *Phys. Biol.* 10: 035005.
26. Rosenfeld, A. M., W. Meng, D. Y. Chen, B. Zhang, T. Granot, D. L. Farber, U. Hershberg, and E. T. Luning Prak. 2018. Computational evaluation of B-Cell clone sizes in bulk populations. *Front. Immunol.* 9: 1472.
27. Choi, Y. S., J. A. Gullicksrud, S. Xing, Z. Zeng, Q. Shan, F. Li, P. E. Love, W. Peng, H. H. Xue, and S. Crotty. 2015. LEF-1 and TCF-1 orchestrate T(FH) differentiation by regulating differentiation circuits upstream of the transcriptional repressor Bcl6. *Nat. Immunol.* 16: 980–990.
28. Yu, D., S. Rao, L. M. Tsai, S. K. Lee, Y. He, E. L. Sutcliffe, M. Srivastava, M. Linterman, L. Zheng, N. Simpson, et al. 2009. The transcriptional repressor Bcl-6 directs T follicular helper cell lineage commitment. *Immunity* 31: 457–468.
29. Chtanova, T., S. G. Tangye, R. Newton, N. Frank, M. R. Hodge, M. S. Rolph, and C. R. Mackay. 2004. T follicular helper cells express a distinctive transcriptional profile, reflecting their role as non-Th1/Th2 effector cells that provide help for B cells. *J. Immunol.* 173: 68–78.
30. Choi, Y. S., R. Kageyama, D. Eto, T. C. Escobar, R. J. Johnston, L. Monticelli, C. Lao, and S. Crotty. 2011. ICOS receptor instructs T follicular helper cell versus effector cell differentiation via induction of the transcriptional repressor Bcl6. *Immunity* 34: 932–946.
31. Boddupalli, C. S., S. Nair, S. M. Gray, H. N. Nowyhed, R. Verma, J. A. Gibson, C. Abraham, D. Narayan, J. Vasquez, C. C. Hedrick, et al. 2016. ABC transporters and NR4A1 identify a quiescent subset of tissue-resident memory T cells. *J. Clin. Invest.* 126: 3905–3916.
32. Tasaki, S., K. Suzuki, A. Nishikawa, Y. Kassai, M. Takiguchi, R. Kurisu, Y. Okuzono, T. Miyazaki, M. Takeshita, K. Yoshimoto, et al. 2017. Multiomic disease signatures converge to cytotoxic CD8 T cells in primary Sjögren's syndrome. *Ann. Rheum. Dis.* 76: 1458–1466.
33. Subramanian, A., P. Tamayo, V. K. Mootha, S. Mukherjee, B. L. Ebert, M. A. Gillette, A. Paulovich, S. L. Pomeroy, T. R. Golub, E. S. Lander, and J. P. Mesirov. 2005. Gene set enrichment analysis: a knowledge-based approach for interpreting genome-wide expression profiles. *Proc. Natl. Acad. Sci. USA* 102: 15545–15550.
34. van der Matten, L., and G. Hinton. 2008. Visulazing data using t-SNEJ. *Mach. Learn. Res.* 9: 2579–2605.
35. Boudousquié, C., M. Danilo, L. Pousse, B. Jeevan-Raj, G. S. Angelov, V. Chennupati, D. Zehn, and W. Held. 2014. Differences in the transduction of canonical Wnt signals demarcate effector and memory CD8 T cells with distinct recall proliferation capacity. *J. Immunol.* 193: 2784–2791.
36. Okhrimenko, A., J. R. Grün, K. Westendorf, Z. Fang, S. Reinke, P. von Roth, G. Wassilew, A. A. Kühl, R. Kudernatsch, S. Demski, et al. 2014. Human memory T cells from the bone marrow are resting and maintain long-lasting systemic memory. *Proc. Natl. Acad. Sci. USA* 111: 9229–9234.
37. Nish, S. A., K. D. Zens, R. Kratchmarov, W. W. Lin, W. C. Adams, Y. H. Chen, B. Yen, N. J. Rothman, A. Bhandoola, H. H. Xue, et al. 2017. CD4+ T cell effector commitment coupled to self-renewal by asymmetric cell divisions. *J. Exp. Med.* 214: 39–47.
38. Buggert, M., S. Nguyen, G. Salgado-Montes de Oca, B. Bengsch, S. Darko, A. Ransier, E. R. Roberts, D. Del Alcazar, I. B. Brody, L. A. Vella, et al. 2018. Identification and characterization of HIV-specific resident memory $CD8^+$ T cells in human lymphoid tissue. *Sci. Immunol.* 3: eaar4526.
39. Busch, D. H., S. P. Fräßle, D. Sommermeyer, V. R. Buchholz, and S. R. Riddell. 2016. Role of memory T cell subsets for adoptive immunotherapy. *Semin. Immunol.* 28: 28–34.
40. June, C. H., R. S. O'Connor, O. U. Kawalekar, S. Ghassemi, and M. C. Milone. 2018. CAR T cell immunotherapy for human cancer. *Science* 359: 1361–1365.